PROCEEDINGS OF SCIENCE

Transverse Single Spin Asymmetry for Inclusive and Diffractive Electromagnetic Jets at Forward Rapidity in $p^{\uparrow}+p$ Collisions at $\sqrt{s}$ = 200 GeV and 510 GeV at STAR

Xilin Liang[a,*] **for STAR collaboration**

[a] *University of California, Riverside,*
900 University Ave, Riverside, CA, USA

E-mail: xlian046@ucr.edu

There have been numerous attempts, in the last decades, to unravel the origin of the unexpectedly significant transverse single-spin asymmetry (A_N) observed in inclusive hadron productions at forward rapidities in transversely polarized $p^{\uparrow}+p$ collisions across various center-of-mass energies ($\sqrt{s}$). The theoretical frameworks that explain this puzzle include the twist-3 contributions in the collinear factorization framework, the transverse-momentum-dependent contributions from the initial-state quark and gluon Sivers functions, and/or final-state Collins fragmentation functions. Recent studies at STAR have also suggested that the prominent A_N values may potentially arise from diffractive processes. We present detailed investigations into the A_N for electromagnetic jets (EM-jets) produced in inclusive processes using the Forward Meson Spectrometer with transversely polarized $p^{\uparrow}+p$ data at $\sqrt{s}$ = 200 GeV collected in 2015 at STAR. Additional studies are performed in order to isolate contributions from diffractive processes to the large inclusive A_N. However, the negative and non-zero A_N is observed for EM-jets in diffractive processes, which can not prove that the large A_N in inclusive processes might come from diffractive processes. Finally, we present the statistical projections of the A_N for inclusive and diffractive EM-jets utilizing $p^{\uparrow}+p$ data at $\sqrt{s}$ = 510 GeV collected in 2017 at STAR. This dataset provides complementary measurements at a high value of $\sqrt{s}$ with a substantial enhancement in statistical precision.

25th International Spin Physics Symposium (SPIN 2023)
24-29 September 2023
Durham, NC, USA

*Speaker

PoS(SPIN2023)032

1. Introduction

Transverse single-spin asymmetry (A_N) is also known as the left-right asymmetry of the particles produced concerning the plane defined by the momentum and spin directions of the polarized beam. In recent decades, various studies have shown this asymmetry in charged- and neutral-hadron productions from polarized hadron-hadron collisions to be large [1–5]. This contradicts nearly zero asymmetry predicted by perturbative Quantum Chromodynamics in the hard scattering processes [6]. Two major recognized frameworks provide potential explanations for such sizeable asymmetries, including the transverse-momentum dependent formalism and the twist-3 factorization scheme. The former introduces contributions from the initial-state quark and gluon Sivers functions and/or the final-state Collins fragmentation functions [7, 8]. The Sivers effect shows that this asymmetry could come from the correlation between the proton spin and the parton's transverse momentum at the initial state [7], while the Collins effect arises from the correlation between the spin of the fragmenting quark and the transverse momentum of the resulting hadron at the final state [8]. The latter includes the contributions from the quark-gluon or gluon-gluon correlations and fragmentation functions [9]. However, recent analyses of A_N for forward π^0 and electromagnetic jets (EM-jets) at STAR indicate that the significant A_N might arise from diffractive processes[5, 10].

The STAR experiment is a major experiment at the Relativistic Heavy Ion Collider (RHIC) at Brookhaven National Laboratory. RHIC is the only polarized proton-proton collider in the world that can provide transversely or longitudinally polarized proton-proton collisions at $\sqrt{s}$ = 200 GeV and 500/510 GeV. In 2015 and 2017, STAR collected high luminosity data with transversely polarized $p^{\uparrow}$ + p collisions at $\sqrt{s}$ = 200 GeV and 510 GeV, respectively. Their average beam polarizations are about 57% and 55%, and their integrated luminosities are about 52 pb^{-1} and 350 pb^{-1}, respectively.

One of the crucial instruments employed for investigating the A_N at forward rapidities is the Forward Meson Spectrometer (FMS). Functioning as an electromagnetic calorimeter, the FMS is specifically designed to capture photons, neutral pions, and η mesons, providing full azimuthal coverage and spanning the pseudo-rapidity range of 2.6 to 4.2 [11] on the west side of STAR apparatus. The Roman Pot detectors (RP) are responsible for detecting slightly scattered protons in close proximity to the beamline [12]. They are located on both the east side and the west side of the STAR apparatus. Additionally, the Beam-Beam Counter (BBC), Vertex Position Detector (VPD), and Zero Degree Calorimeter (ZDC) served roles in data triggering as well as determining the primary vertex [13].

2. Inclusive EM-jet A_N for $p^{\uparrow}$ + p data at $\sqrt{s}$ = 200 GeV

The EM-jet is the EM component of a full jet. The photon candidates used for reconstructing the EM-jets were the FMS points, where the details for FMS points can be found in [5]. The anti-k_T algorithm was employed to reconstruct the EM-jets, with a resolution parameter of R = 0.7 [14]. Depending on the analyzed dataset, the minimum transverse momentum (p_T) requirement for the EM-jets was determined by either the trigger threshold or a fixed threshold.

The reconstructed EM-jet energy and transverse momentum (p_T) underwent a correction process where the underlying event contribution was subtracted via the "off-axis" cone method

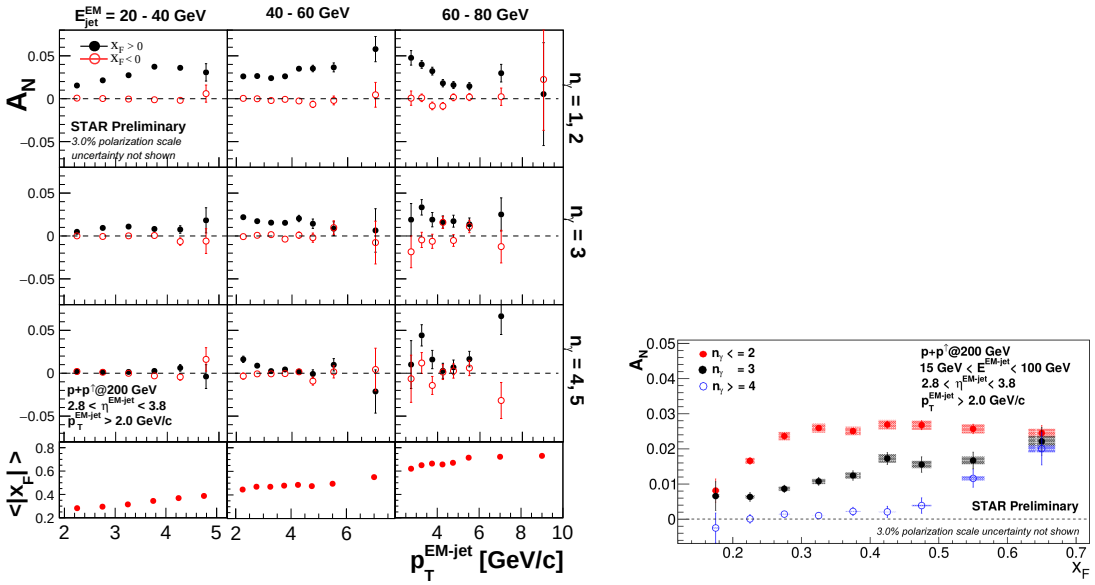

Figure 1: (left) A_N of inclusive EM-jet at $\sqrt{s}$ = 200 GeV sorted by EM-jet photon multiplicity, p_T, and energy bins. The lowermost panels display the average x_F values corresponding to each p_T bin. The black solid points represent the A_N values for $x_F > 0$ and the red hollow points depict the A_N values for $x_F < 0$. (right) Inclusive EM-jet A_N as a function of x_F at $\sqrt{s}$ = 200 GeV for three cases: $n_\gamma \leq 2$, $n_\gamma = 3$, $n_\gamma \geq 4$.

[15]. Subsequently, to align the EM-jet kinematics with the "particle level", corrections based on simulations were applied to accommodate the detector effect. The simulation framework was set up with PYTHIA 6 with Perugia 2012 Tune for the particle level event generation [16, 17]. The generated events were then passed through the GEANT-based STAR detector simulation.

The cross-ratio method was used to extract the A_N [18]. The left panel of Fig. 1 presents the preliminary results of the inclusive EM-jet A_N as a function of photon multiplicity, EM-jet p_T, and EM-jet energy. For $x_F < 0$ (where x_F denotes the longitudinal momentum fraction $x_F = 2p_L/\sqrt{s}$), the A_N for the EM-jet decreases as the photon multiplicity of the EM-jets increases. Furthermore, the observed A_N remains consistent with zero across varying photon multiplicities for $x_F < 0$.

The right panel of Fig. 1 delves into a detailed exploration of the inclusive EM-jet A_N as a function of x_F with a dependency on EM-jet photon multiplicity. Overall, the inclusive EM-jet A_N shows an increasing trend as x_F increases, regardless of the photon multiplicity. Noteworthy is the observation that EM-jets composed of 1 or 2 photons exhibit the most prominent asymmetry in both figures. These findings suggest that substantial contributions to the significant A_N may originate from diffractive processes.

3. Diffractive EM-jet A_N for $p^{\uparrow} + p$ data at $\sqrt{s}$ = 200 GeV

Two possible channels are considered diffractive processes. In the first channel, the scenario involves the presence of an EM-jet at the FMS alongside only one proton track at the west-side RP, with the absence of any proton track at the east-side RP. Conversely, the second channel necessitates the existence of an EM-jet at the FMS, accompanied by only one proton track at both the west and

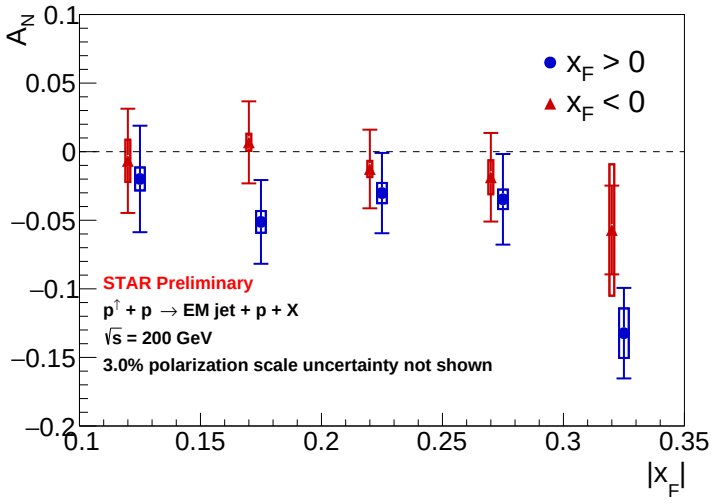

Figure 2: Diffractive EM-jet A_N as a function of x_F at $\sqrt{s}$ = 200 GeV. The blue points represent $x_F > 0$, while the red points represent $x_F < 0$ with a constant shift of -0.005 along the x-axis for clarity. The rightmost points correspond to $0.3 < |x_F| < 0.45$.

east side RPs. The reconstruction and corrections for EM-jets in these diffractive processes parallel those employed in inclusive processes, as detailed in Section 2. The number of proton tracks detected on each side of RP must conform to the specifications for either of the defined channels. Also, those detected proton tracks must be appropriately reconstructed based on the geometric acceptance of the RP.

In high luminosity collisions, the presence of substantial background contamination, such as accidental coincidences, posed a significant challenge. Consequently, to minimize those effects, additional selection criteria were applied. The cut based on the ADC value of west-side BBC was employed. Only events with BBC ADC values below the specified threshold were retained. Furthermore, the sum energy, calculated as the sum of the energy from the west side RP track and the FMS EM-jets, exceeded a predetermined threshold was excluded from the analysis. More comprehensive information on these event selection criteria can be found in [18].

The cross-ratio method was used to extract the A_N for diffractive process. Figure 2 presents the preliminary result for diffractive EM-jet A_N as a function of x_F. We observe a non-zero diffractive EM-jet A_N with a significance of 3.3σ below 0 at forward rapidity ($x_F > 0$), while the A_N for $x_F < 0$ is found to be consistent with zero. Moreover, a significant absolute A_N is observed at the high x_F region. However, the sign of the diffractive EM-jet A_N is negative, which stands in contrast to the inclusive EM-jet A_N in Fig. 1. The diffractive EM-jet A_N does not exhibit indications of contributing to the larger A_N values observed in the inclusive processes. More theoretical inputs are needed to understand the behavior observed in the diffractive results.

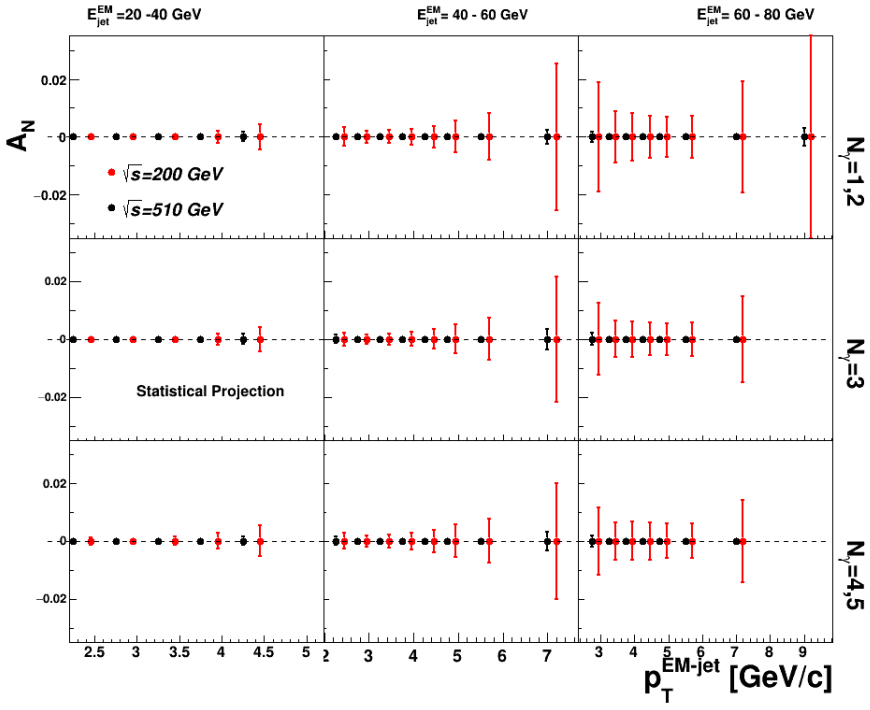

Figure 3: Statistical projections for inclusive processes for $p^{\uparrow}$ + p collisions at $\sqrt{s}$ = 510 GeV (black) compared to results at $\sqrt{s}$ = 200 GeV (red) at STAR.

4. Statistical projections for $p^{\uparrow}$+ p data at $\sqrt{s}$ = 510 GeV

The ongoing analyses of A_N for both inclusive and diffractive processes are being conducted using $p^{\uparrow}$+ p collision data at $\sqrt{s}$ = 510 GeV. This high luminosity dataset presents promising prospects for a more precise investigation of A_N in both inclusive and diffractive scenarios. To illustrate the anticipated improvements, the statistical projection plots for the inclusive processes (Fig. 3) and the diffractive process (Fig. 4) are presented with the comparison between the datasets at $\sqrt{s}$ = 200 GeV and 510 GeV. With the utilization of the $\sqrt{s}$ = 510 GeV data, a significant improvement in the precision of A_N measurements is expected, resulting in a remarkable reduction in statistical uncertainty by about a factor of 3 for the EM-jets exhibiting high energy and high photon multiplicity in inclusive measurements. Furthermore, a reduction by more than a factor of 2 is expected for diffractive EM-jet A_N measurements.

5. Conclusion

We present the A_N for inclusive and diffractive EM-jet using the FMS at STAR in $p^{\uparrow}$ + p collisions at $\sqrt{s}$ = 200 GeV. The inclusive EM-jet A_N exhibits an increasing trend with higher values of x_F and decreasing photon multiplicity. Notably, the largest was A_N with 1 or 2 photon multiplicity for the inclusive processes. The A_N for the diffractive processes is shown to be non-zero with a significance of 3.3 σ. However, the sign of diffractive A_N is negative, opposite to

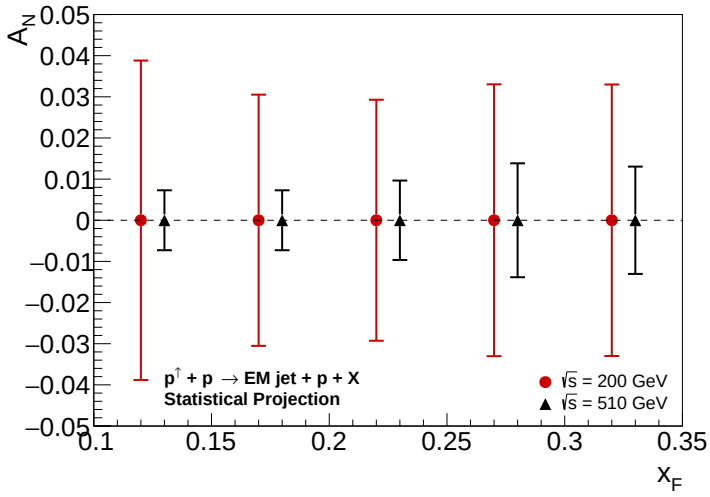

Figure 4: Statistical projections for diffractive processes for $p^{\uparrow} + p$ collisions at $\sqrt{s}$ = 510 GeV (black) compared to results at $\sqrt{s}$ = 200 GeV (red) at STAR.

that observed in the inclusive processes. Further theoretical inputs are needed to understand its underlying physics. Finally, with the higher luminosity data set for $p^{\uparrow} + p$ collisions at $\sqrt{s}$ = 510 GeV at STAR, a higher precision will be achieved for both the inclusive and diffractive EM-jet A_N.

References

[1] D.L. Adams *et al.*, Phys. Lett. B 261, 201(1991)

[2] B. I. Abelev *et al.* (STAR Collaboration), Phys. Rev. Lett. 101, 222001(2008)

[3] A. Adare *et al.* Phys. Rev. D 90, 012006 (2014)

[4] E.C. Aschenauer *et al.*, arXiv:1602.03922

[5] J. Adam *et al.* (STAR Collaboration), Phys. Rev. D 103, 092009 (2021)

[6] G. L. Kane, J. Pumplin, and W. Repko. Phys. Rev. Lett. 41, 1689 (1978)

[7] D. Sivers, Phys. Rev. D 41, 83 (1990)

[8] J. Collins, Nucl Phys B 396 (1993) 161

[9] J.W. Qiu and G. Sterman, Phys. Rev. Lett. 67 2264 (1991)

[10] M.M. Mondal (STAR Collaboration) PoS (DIS2014) 216

[11] J. Adam *et al.* (STAR Collaboration), Phys. Rev. D 98, 032013 (2018)

[12] J. Adam *et al.* (STAR Collaboration), Phys. Lett. B 808 (2020) 135663

[13] K. H. Ackermann *et al.* (STAR Collaboration), Nucl. Instrum. Meth. A 499, 624-632 (2003).

[14] M.Cacciari, G. P. Salam, and G. Soyez, Eur. Phys. J. C (2012) 72: 1896

[15] B. B. Abelev *et al.* (ALICE Collaboration), Phys. Rev. D 91, 112012 (2015)

[16] T. Sjostrand, S. Mrenna, and P. Z. Skands, JHEP 05, 026 (2006)

[17] Peter Z. Skands Phys. Rev. D 82, 074018

[18] X. Liang (STAR Collaboration) 10.5281/zenodo.7236716